REPORT DOCUMENTATION PAGE

Form Approved
OMB No. 0704-0188

1. REPORT DATE *(DD-MM-YYYY)*
December 2014

2. REPORT TYPE
Briefing Chart

3. DATES COVERED *(From - To)*
December 2014- January 2015

4. TITLE AND SUBTITLE
Comparison of a Structured-LES and an Unstructured-DES Code for Predicting Combustion Instabilities in a Longitudinal Mode Rocket

5a. CONTRACT NUMBER
In-House

5b. GRANT NUMBER

5c. PROGRAM ELEMENT NUMBER

6. AUTHOR(S)
Matt Harvazinski, Doug Talley, Venke Sankaran

5d. PROJECT NUMBER

5e. TASK NUMBER

5f. WORK UNIT NUMBER
Q0A1

7. PERFORMING ORGANIZATION NAME(S) AND ADDRESS(ES)
Air Force Research Laboratory (AFMC)
AFRL/RQRC
10 E. Saturn Blvd.
Edwards AFB, CA 93524-7680

8. PERFORMING ORGANIZATION REPORT NO.

9. SPONSORING / MONITORING AGENCY NAME(S) AND ADDRESS(ES)
Air Force Research Laboratory (AFMC)
AFRL/RQR
5 Pollux Drive.
Edwards AFB CA 93524-7048

10. SPONSOR/MONITOR'S ACRONYM(S)

11. SPONSOR/MONITOR'S REPORT NUMBER(S)
AFRL-RQ-ED-VG-2014-376

12. DISTRIBUTION / AVAILABILITY STATEMENT
Distribution A: Approved for Public Release; Distribution Unlimited

13. SUPPLEMENTARY NOTES
Briefing Charts presented at AIAA 2015 SciTech, Kissimmee, FL, 8 Jan 2015. PA#15023

14. ABSTRACT
N/A

15. SUBJECT TERMS

16. SECURITY CLASSIFICATION OF:			17. LIMITATION OF ABSTRACT	18. NUMBER OF PAGES	19a. NAME OF RESPONSIBLE PERSON
					Doug Talley
a. REPORT	**b. ABSTRACT**	**c. THIS PAGE**	SAR	28	**19b. TELEPHONE NO** *(include area code)*
Unclassified	**Unclassified**	**Unclassified**			661-275-6174

Standard Form 298 (Rev. 8-98)
Prescribed by ANSI Std. 239.18

THE AIR FORCE RESEARCH LABORATORY
LEAD | DISCOVER | DEVELOP | DELIVER

Comparison of a Structured-LES and an Unstructured-DES Code for Predicting Combustion Instabilities in a Longitudinal Mode Rocket

Matt Harvazinski, Doug Tally, & Venke Sankaran
Air Force Research Laboratory
Edwards AFB, CA

Outline

- Introduction
- Results – Unstable operating point
- Results – Stable operating point
- Summary and Conclusions

History

Combustion instability is an organized, oscillatory motion in a combustion chamber sustained by combustion.

CI caused a four year delay in the development of the F-1 engine used in the Apollo program

> 2000 full scale tests

> $400 million for propellants alone (2010 prices)

Irreparable damage can occur in less than 1 second.

Damaged engine injector faceplate caused by combustion instability

"Combustion instabilities have been observed in almost every engine development effort, including even the most recent development programs"

– JANNAF Stability Panel Draft (2010)

Longitudinal Experiment

Continuously Varying Resonance Chamber

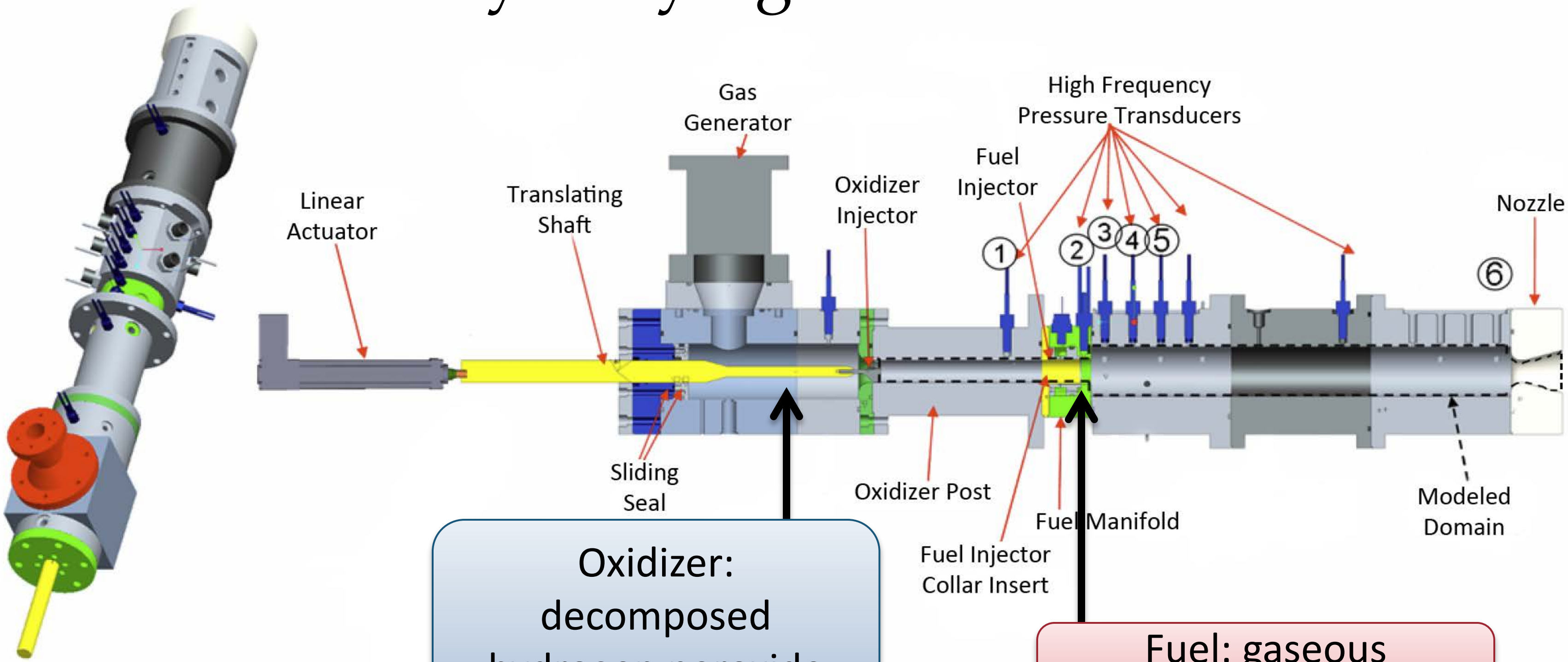

Oxidizer: decomposed hydrogen peroxide

Fuel: gaseous methane

Yu et al. 2013

Experimental Results

Unsteady pressure for a translating test

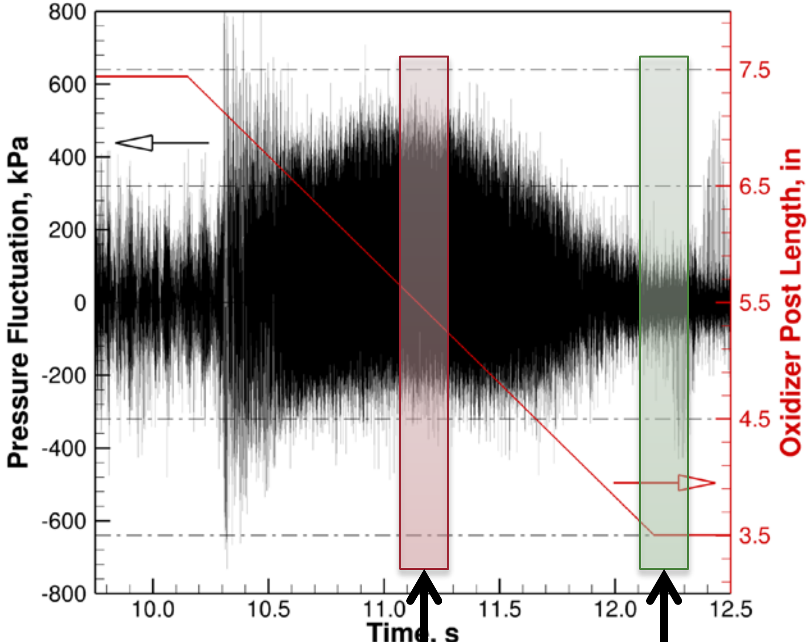

Unstable

Marginally Stable

PSD power for the first mode

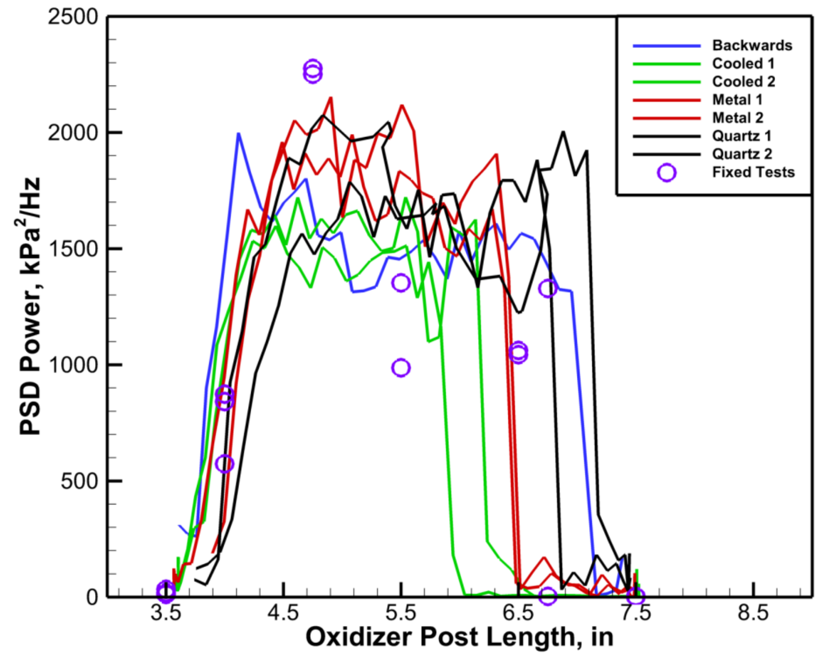

Harvazinski et al. 2013

Instability Mechanism

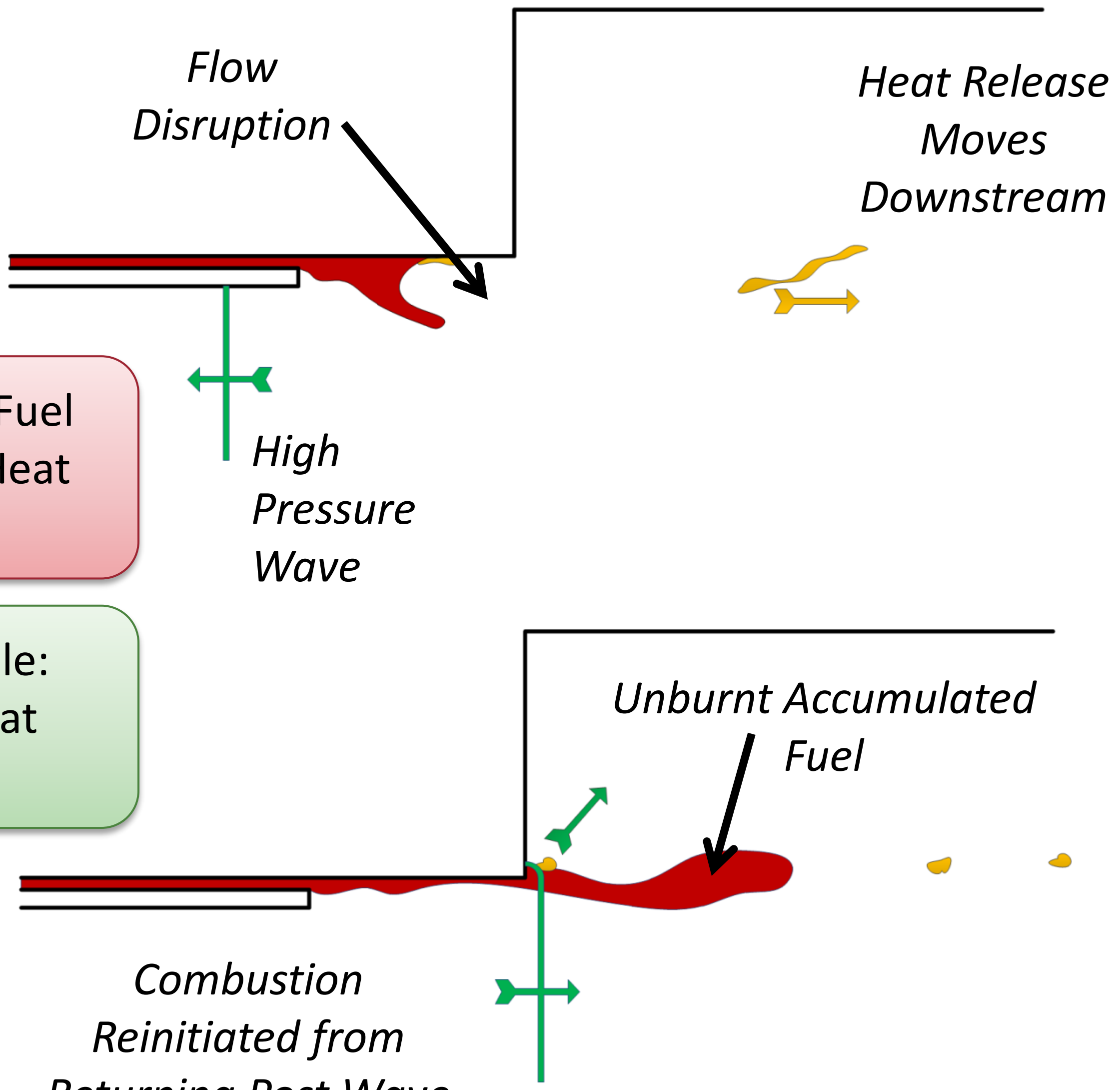

Unstable: Cyclic Fuel Disruption and Heat Release

Marginally Stable: Continuous Heat Release

Distribution A: approved for public release; distribution unlimited.

Complementary Codes

Exercised Code Options:

LESLIE	GEMS
Structured	Unstructured
Explicit MacCormack	Implicit Dual-Time
LES	DES
Laminar Combustion Closure	
Second Order Accurate in Time & Space	

Choked inlet slots have been ignored

2-Step reduced mechanism

LES: 7.3/7.6M

DES: 3.6/4M

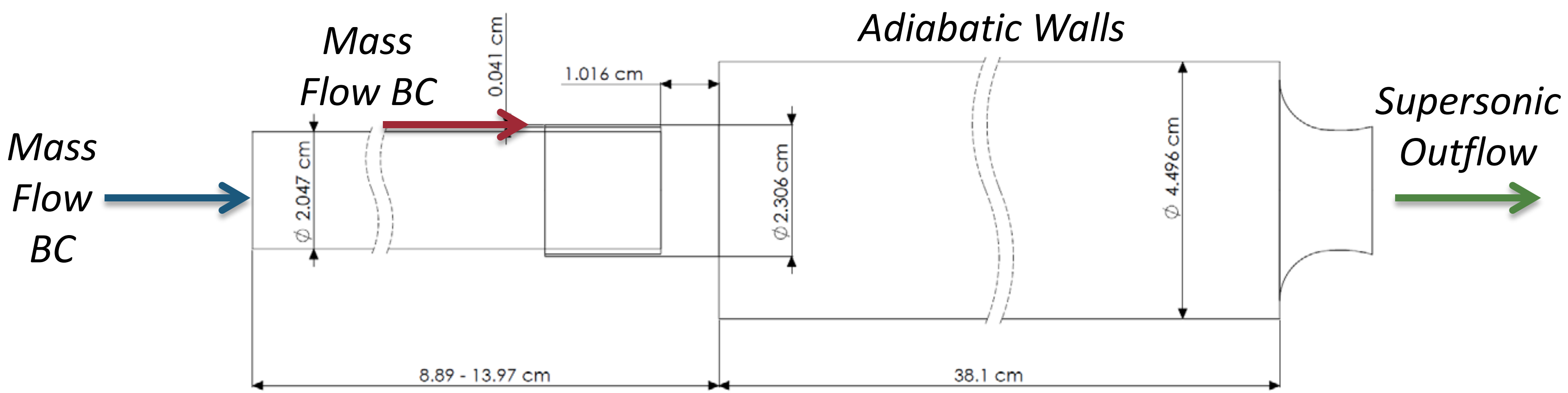

Distribution A: approved for public release; distribution unlimited.

DES Turbulence Model

Modified Wilcox *k*-*ω*

$$\frac{\partial \overline{\rho} k}{\partial t} + \frac{\partial \overline{\rho} \widetilde{u}_j k}{\partial x_j} = \widetilde{\tau}_{ij} \frac{\partial \widetilde{u}_i}{\partial x_j} - \boxed{\beta^\star \overline{\rho} \omega k} + \frac{\partial}{\partial x_j} \left[\left(\mu + \sigma_k \frac{\overline{\rho} k}{\omega} \right) \frac{\partial k}{\partial x_j} \right]$$

$$\frac{\partial \overline{\rho} \omega}{\partial t} + \frac{\partial \overline{\rho} \widetilde{u}_j \omega}{\partial x_j} = \frac{\gamma \omega}{k} \widetilde{\tau}_{ij} \frac{\partial \widetilde{u}_j}{\partial x_j} - \beta \overline{\rho} \omega^2 + \frac{\partial}{\partial x_j} \left[\left(\mu + \sigma_\omega \frac{\overline{\rho} k}{\omega} \right) \frac{\partial \omega}{\partial x_j} \right]$$

The eddy viscosity is reduced by modifying the turbulent length scale

$$L_{\mathrm{T}} = \frac{\sqrt{k}}{\beta^\star \omega} \qquad \boxed{\beta^\star k \omega} = \frac{k^{3/2}}{L_{\mathrm{T}}^\star} \qquad L_{\mathrm{T}}^\star = \min\left(L_{\mathrm{T}}, C_{\mathrm{DES}} \Delta\right)$$

LES Turbulence Model

Solve a transport equation of the sub-grid kinetic energy

$$\frac{\partial \overline{\rho} k^{\mathrm{sgs}}}{\partial t} + \frac{\partial \overline{\rho} \widetilde{u}_i k^{\mathrm{sgs}}}{\partial x_i} = -\tau_{ij}^{\mathrm{sgs}} \frac{\partial \widetilde{u}_i}{\partial x_j} - C_\epsilon \overline{\rho} \frac{(k^{\mathrm{sgs}})^{3/2}}{\Delta} + \frac{\partial}{\partial x_i}\left[\left(\frac{\overline{\rho}\nu_T}{\sigma_k} + \mu\right)\frac{\partial k^{\mathrm{sgs}}}{\partial x_i} + \frac{\overline{\rho}\nu_T R}{\mathrm{Pr}_T}\frac{\partial \widetilde{T}}{\partial x_i}\right]$$

Eddy viscosity is found using a constant model

$$\nu_{\mathrm{T}} = C_\nu \Delta \sqrt{k^{\mathrm{sgs}}}$$

Standard gradient diffusion hypothesis closures

$$\tau_{ij}^{\mathrm{sgs}} = \overline{\rho}\nu_{\mathrm{T}}\left(\frac{\partial \widetilde{u}_i}{\partial x_j} + \frac{\partial \widetilde{u}_j}{\partial x_i} - \frac{2}{3}\frac{\partial \widetilde{u}_k}{\partial x_k}\right) + \frac{2}{3}k^{\mathrm{sgs}}\delta_{ij}$$

Unstable Operating Point

DES

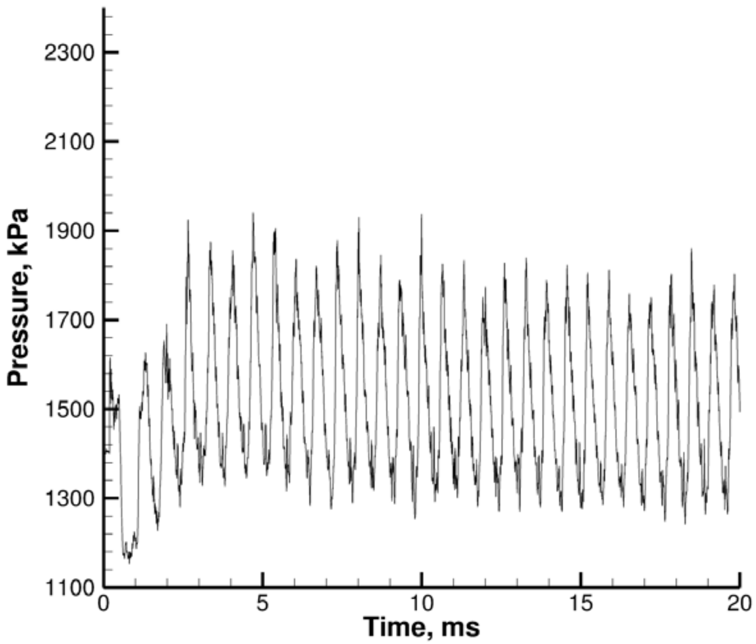

Mean Pressure – 1.5 MPa

LES

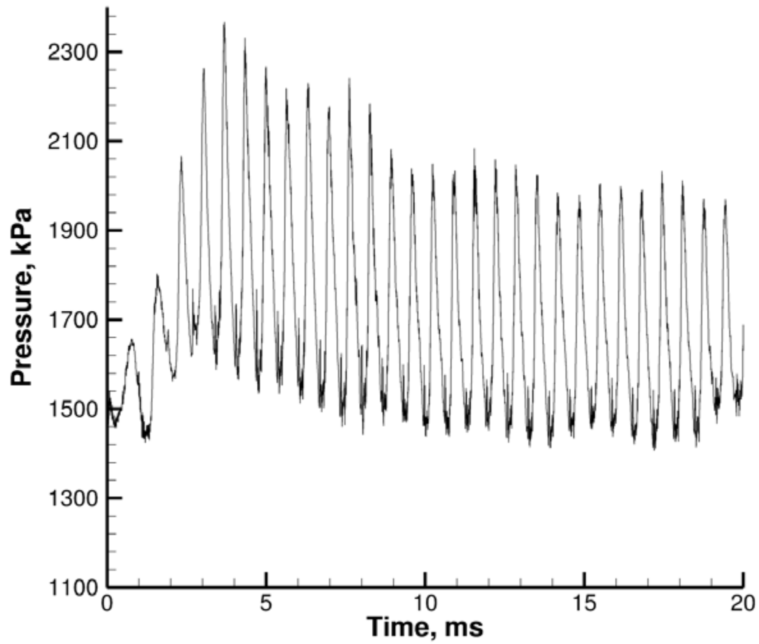

Mean Pressure – 1.7 MPa

Fluctuating Pressure

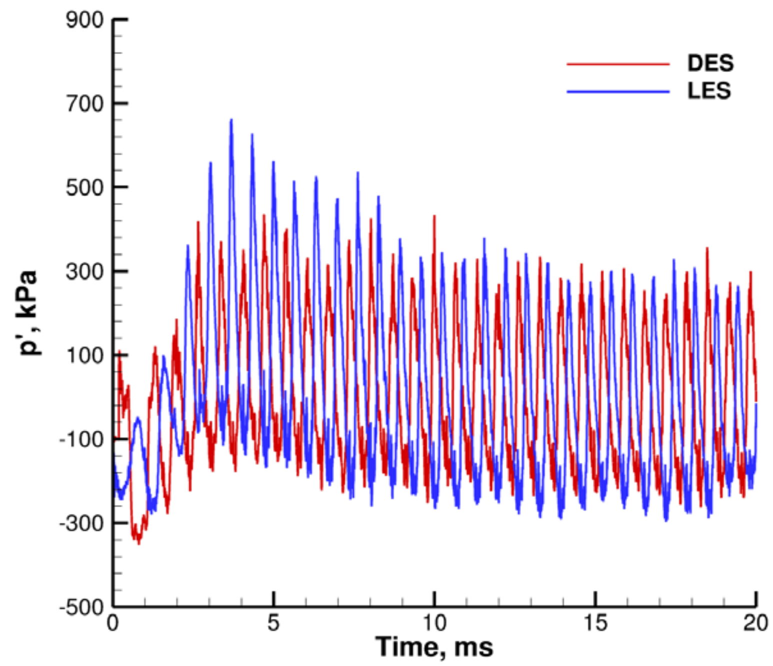

Comparable amplitude and frequency

DES reaches a limit cycle faster

Phase Difference

DES

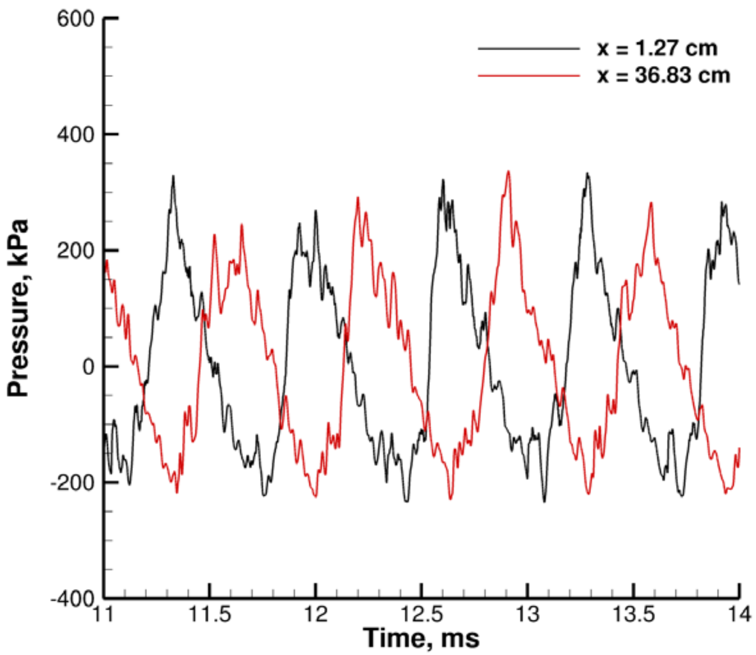

LES

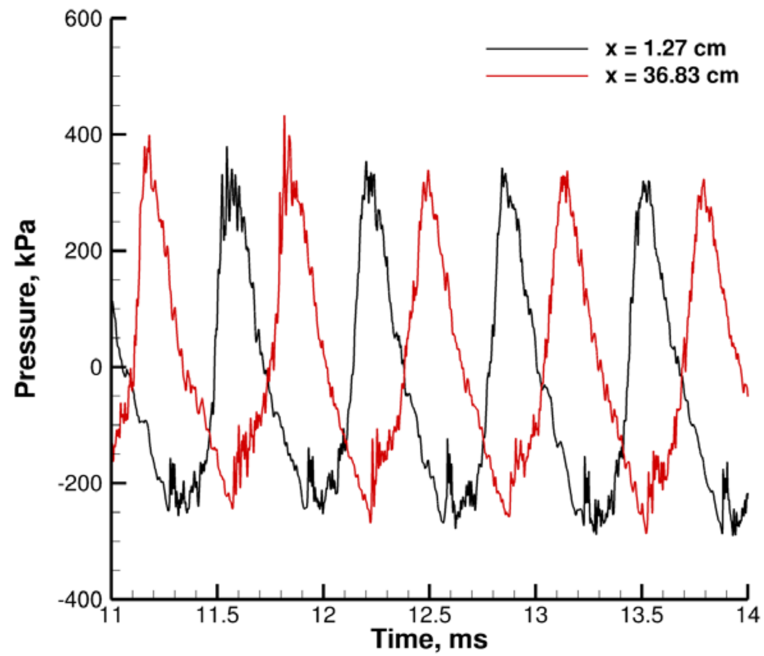

The phase difference between the head end and the downstream end is captured

Integrated PSD Data

Mode	Experiment		DES		LES	
	f, Hz	p'_{ptp}, kPa	f, Hz	p'_{ptp}, kPa	f, Hz	p'_{ptp}, kPa
1	1324	387.15	1500	316.748	1500	382.547
2	2655	89.29	3050	86.677	3050	119.221
3	3979	46.37	4550	50.525	4550	70.507
4	7940	41.97	5700	17.583	6100	16.879
Σ		564.78		471.533		589.154

Similar frequency predictions, both high relative to the experiment

Mode 4 is under predicted for both codes

Higher amplitude for LES for modes 1-3

Unsteady Flowfield – High Pressure

DES

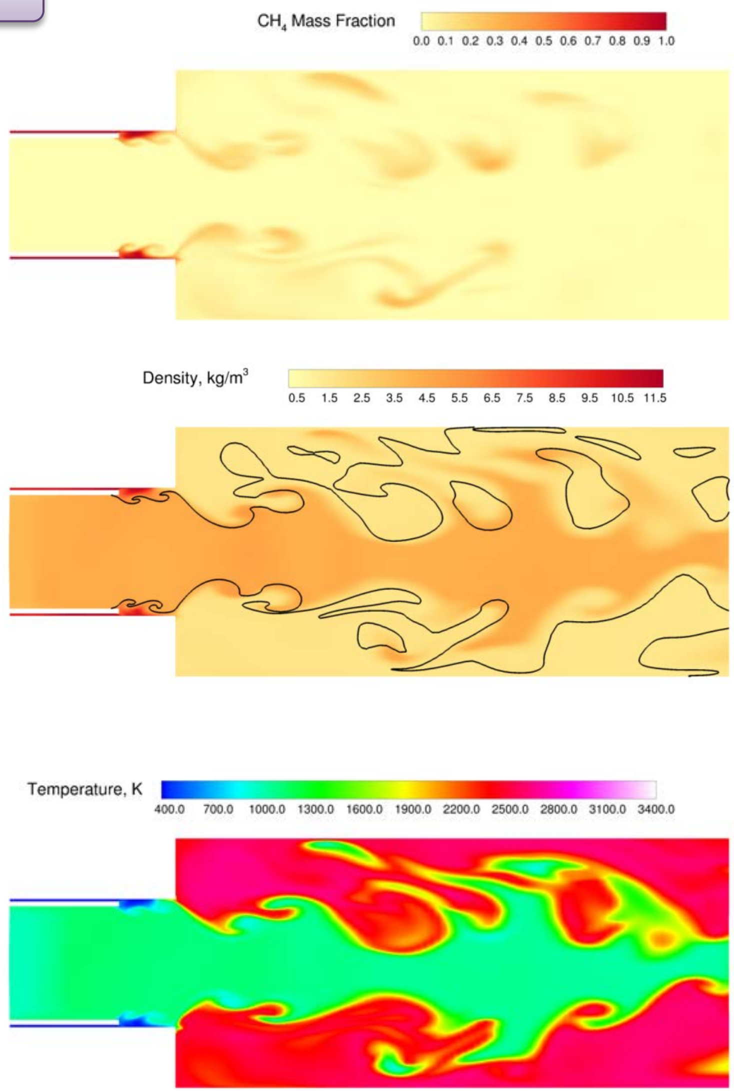

LES

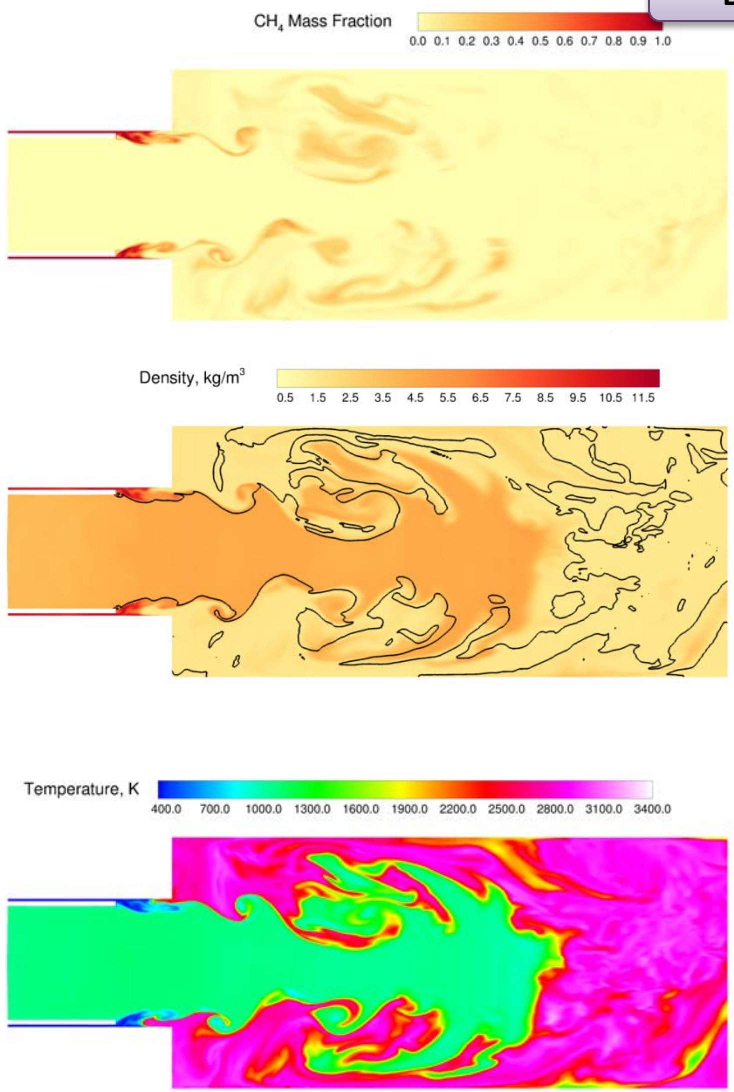

Unsteady Flowfield – Low Pressure

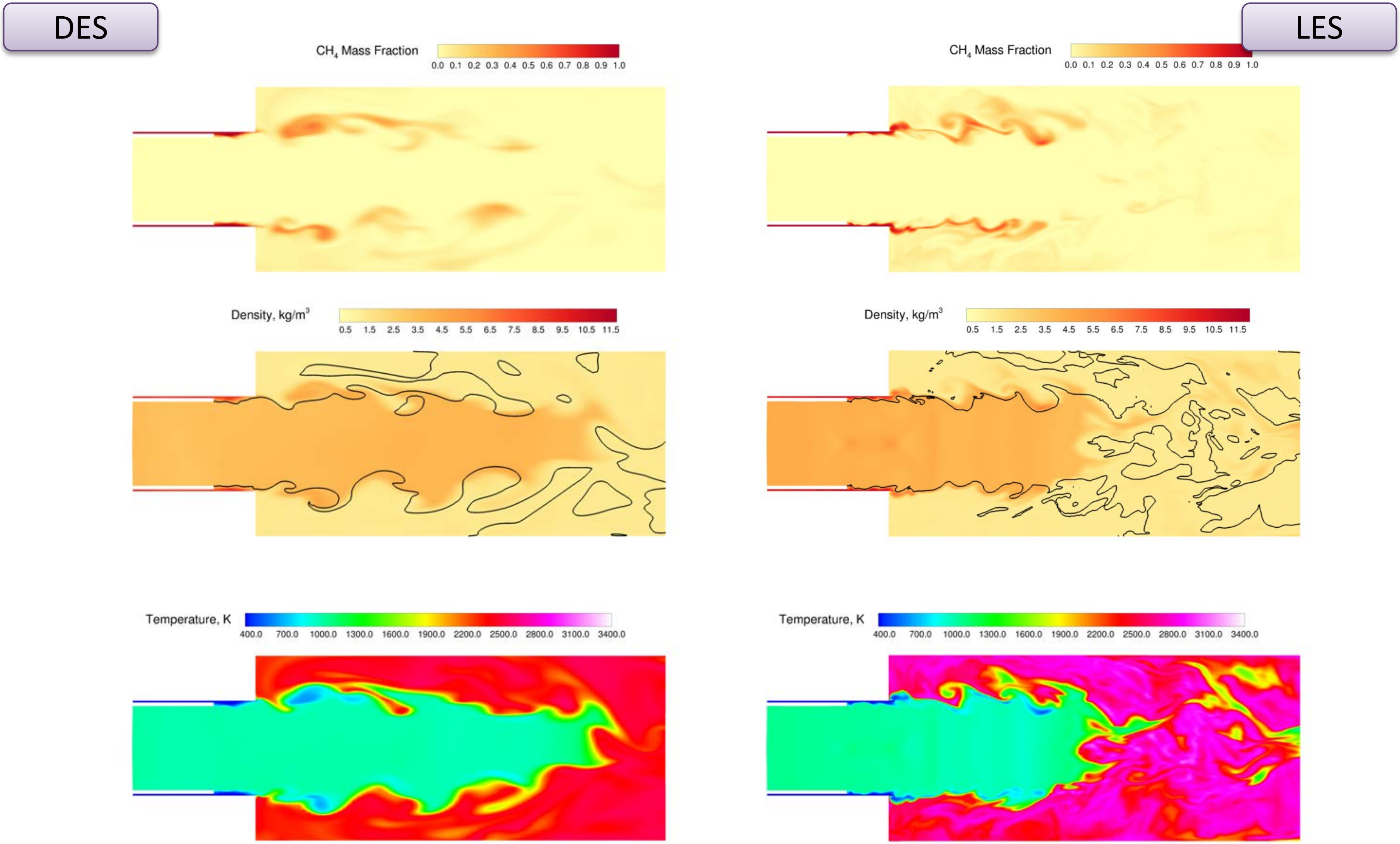

Distribution A: approved for public release; distribution unlimited.

Heat Release Cycle – Part I

DES

Start

LES

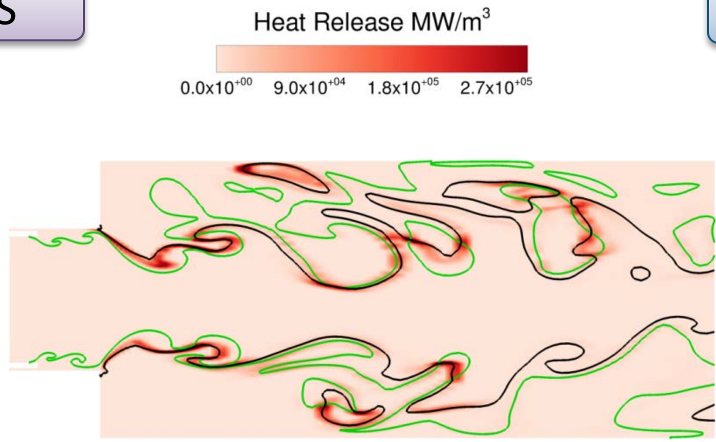

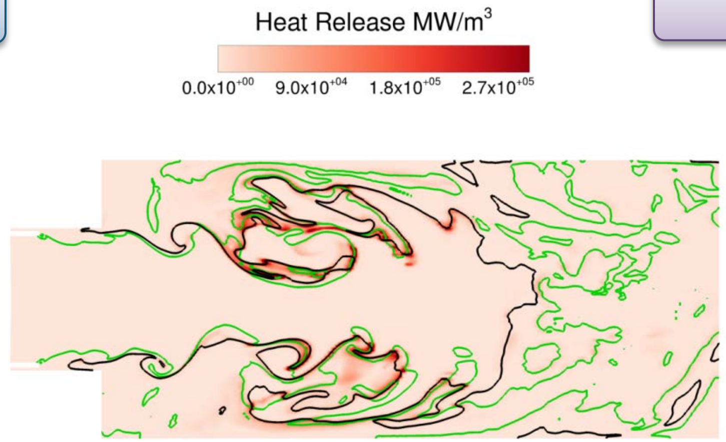

30 %

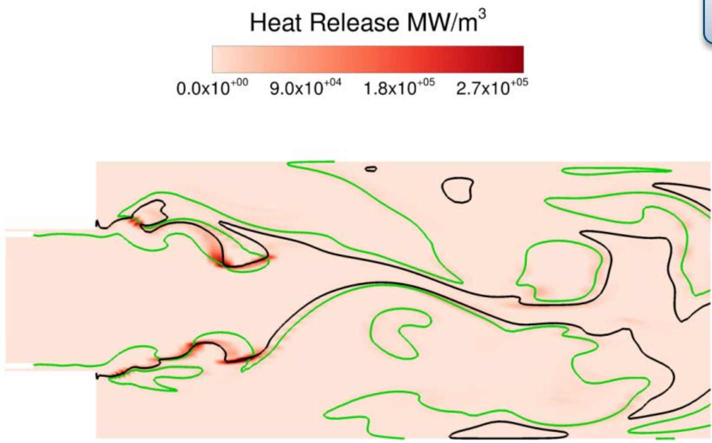

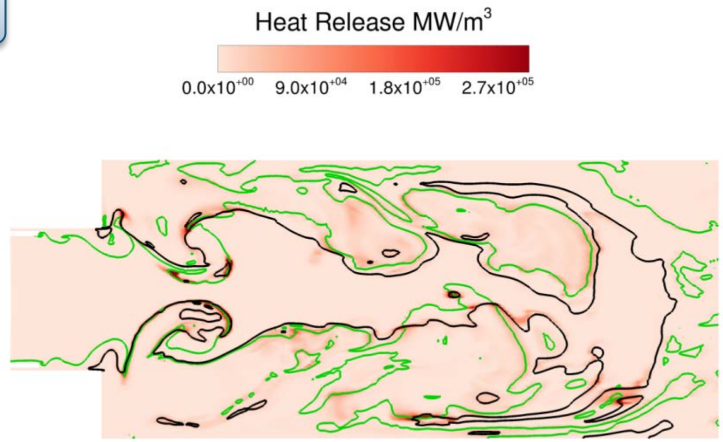

Heat Release Cycle – Part II

DES

60 %

LES

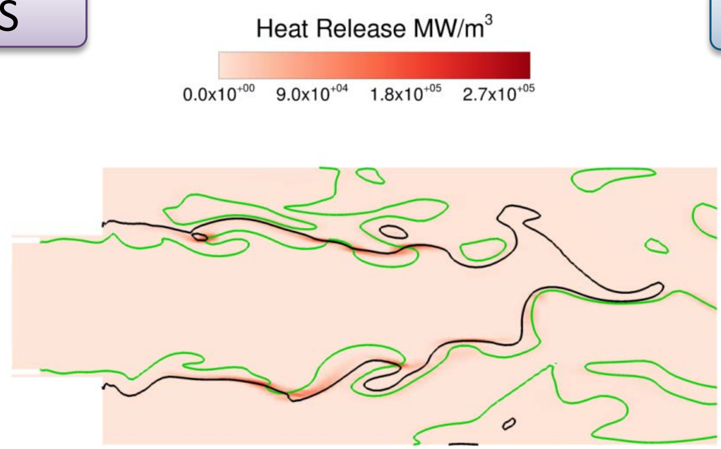

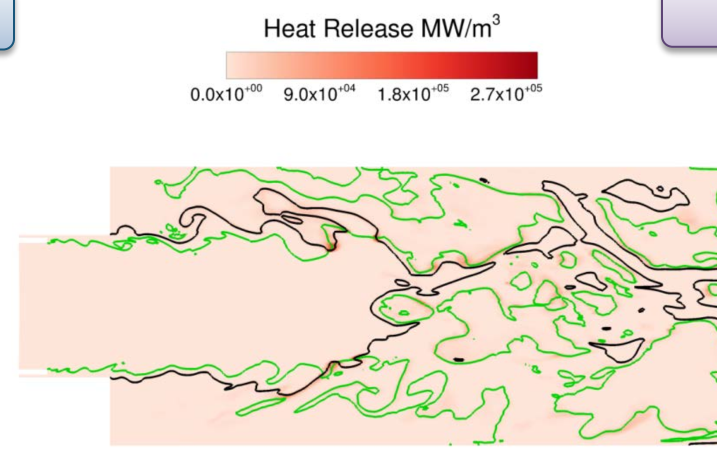

90 %

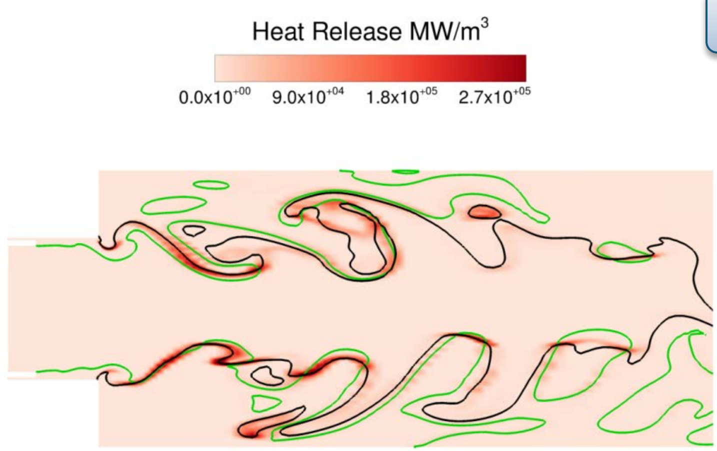

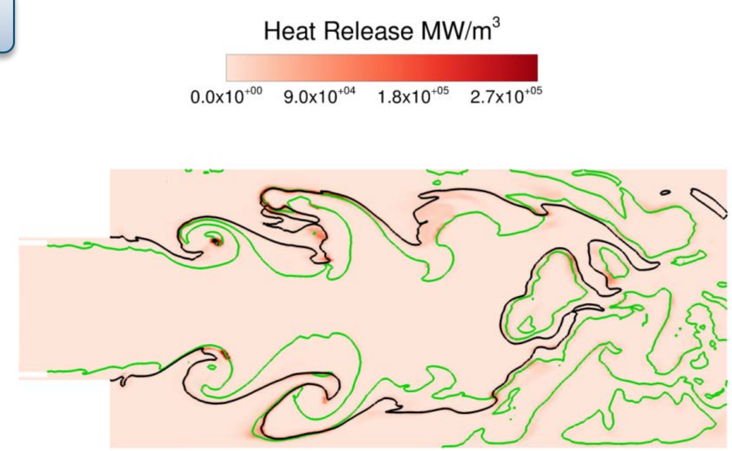

Fuel Cut Off Event

DES

LES

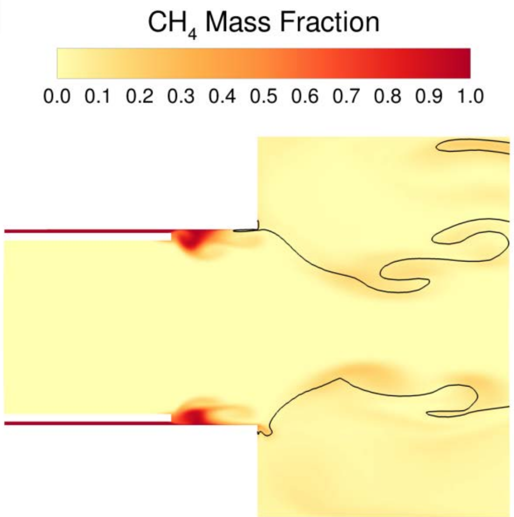

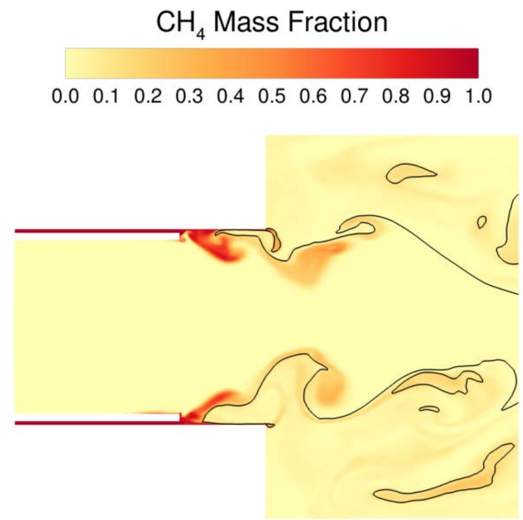

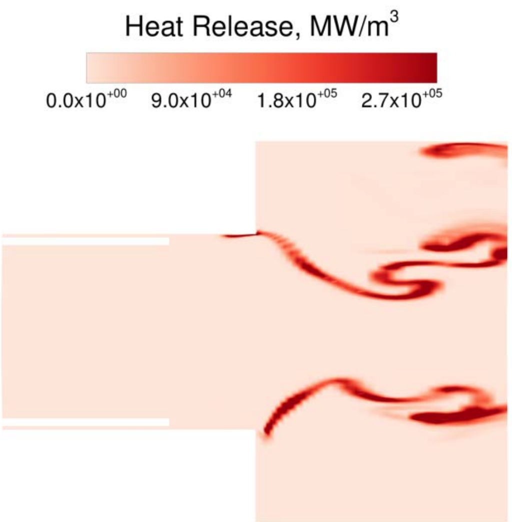

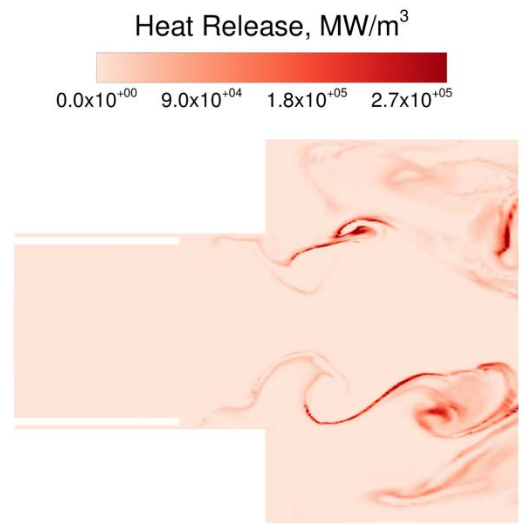

Reignition Event

Qualitative agreement with reignition behavior

Accumulated methane in the shear layer in both cases

LES

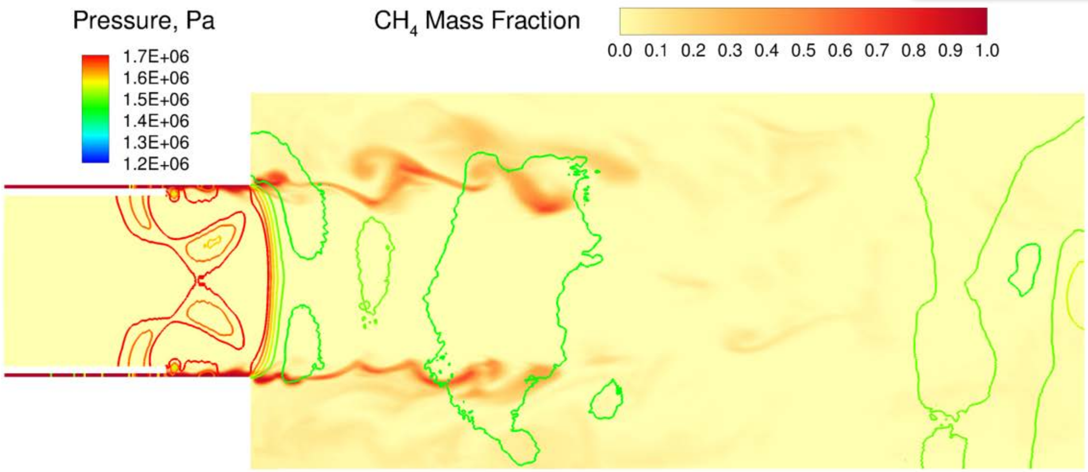

DES

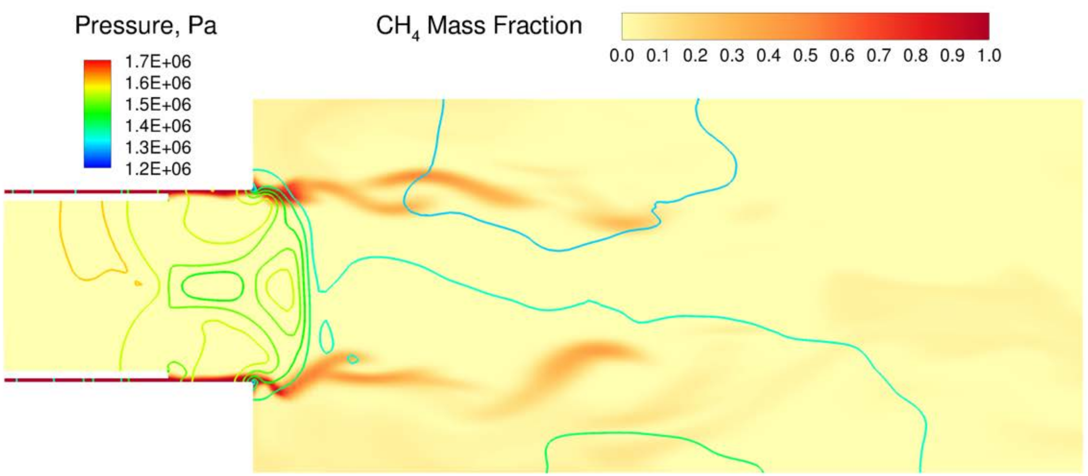

Marginally Stable Operating Point

DES

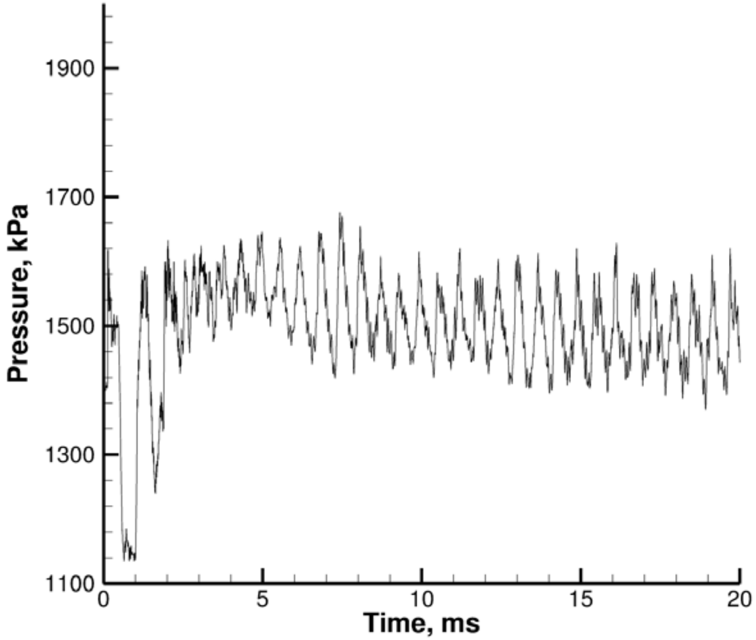

Mean Pressure – 1.5 MPa

LES

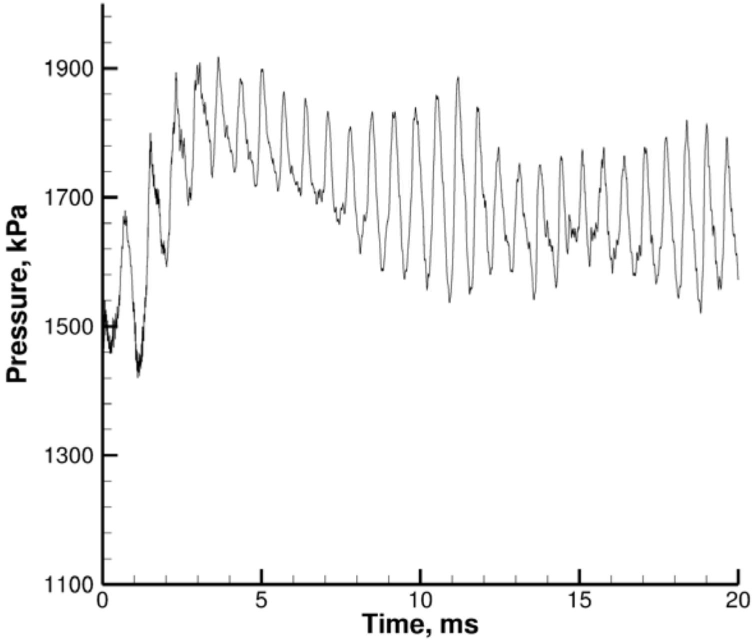

Mean Pressure – 1.7 MPa

Fluctuating Pressure

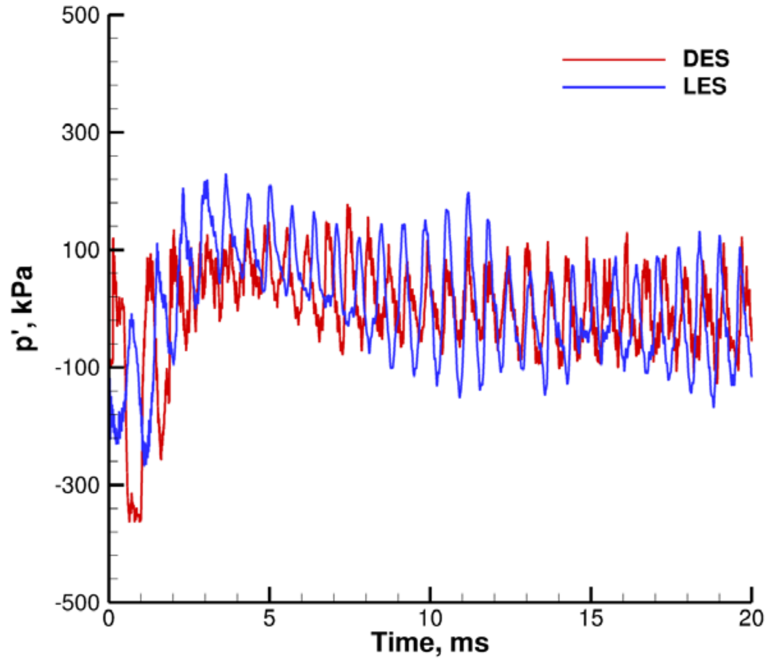

Comparable amplitude and frequency

LES shows more variability

Integrated PSD Data

Mode	Experiment		DES		LES	
	f, Hz	p'_{ptp}, kPa	f, Hz	p'_{ptp}, kPa	f, Hz	p'_{ptp}, kPa
1	1379	121.17	1600	93.527	1500	141.330
2	3881	5.86	3250	23.726	3000	43.698
3	6475	16.03	4050	13.573	4200	9.623
Σ		143.06		130.826		194.651

LES Over predicts total amplitude

Both cases severely over predict the second mode amplitude

Frequency differences

Unsteady Flowfield – High Pressure

DES

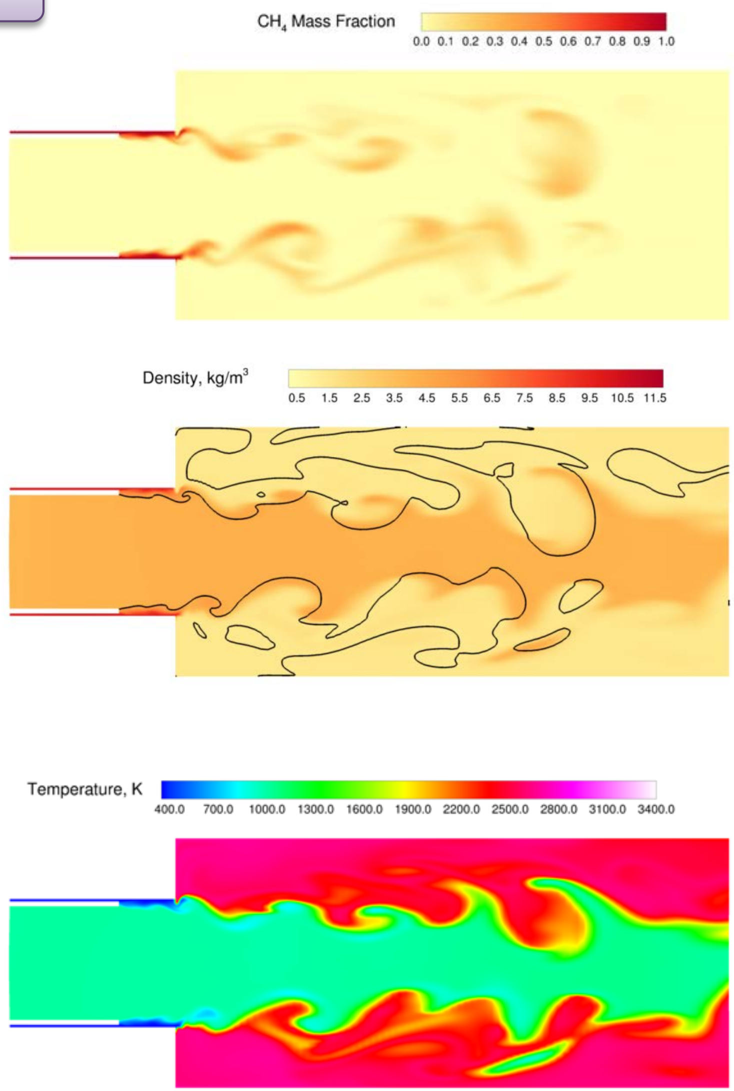

LES

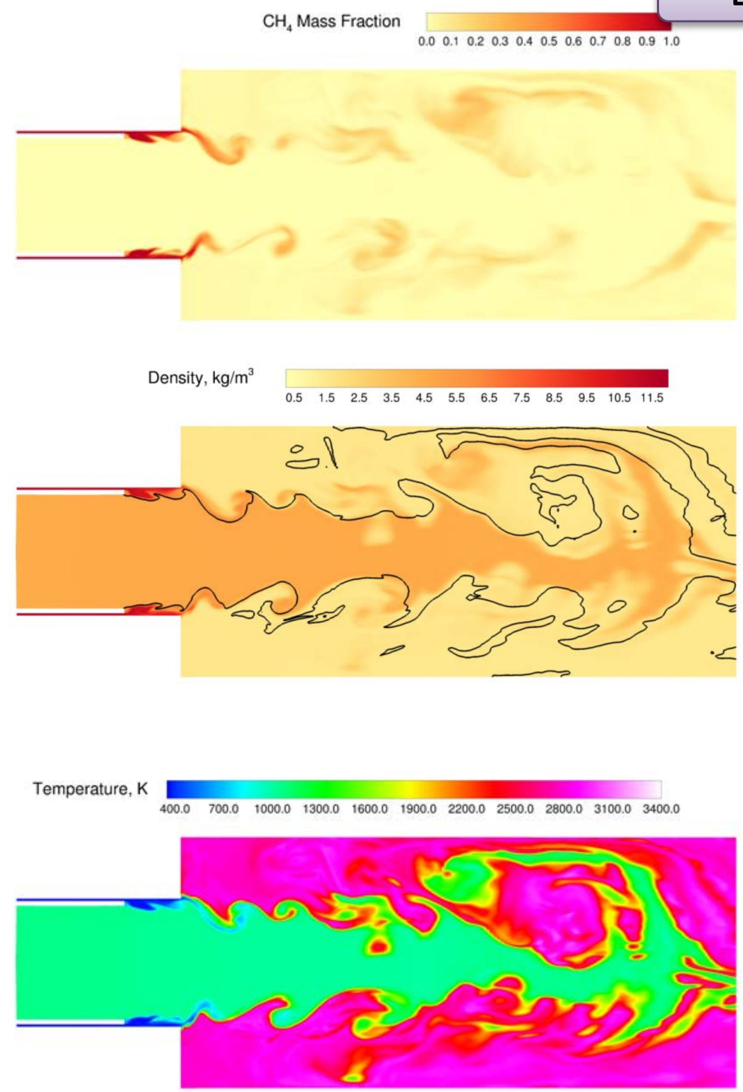

Unsteady Flowfield – Low Pressure

DES

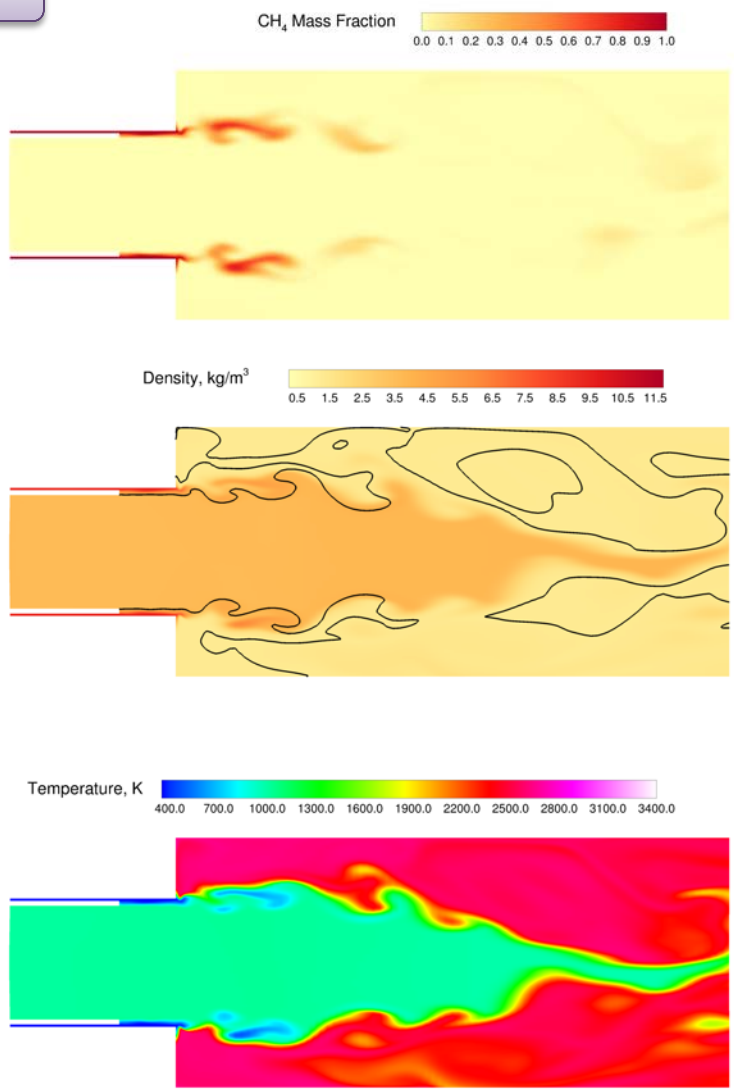

LES

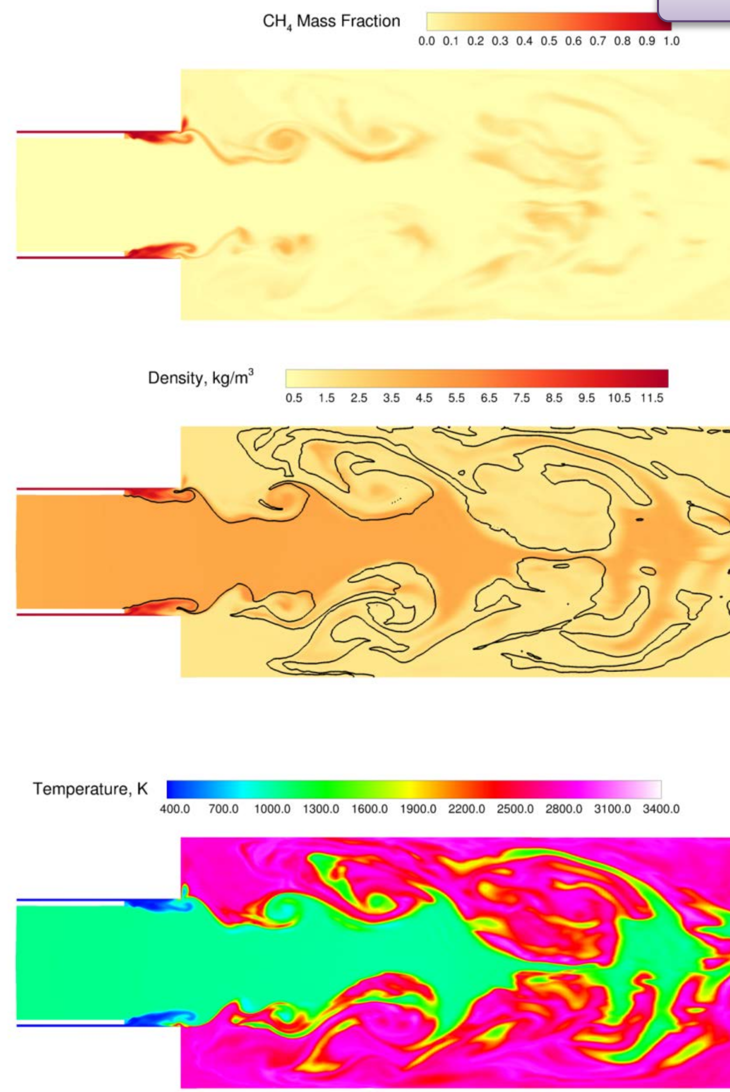

Heat Release Cycle – Part I

DES

Start

LES

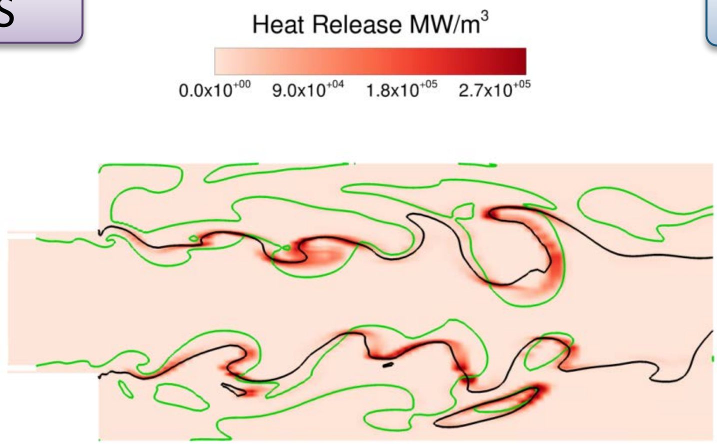

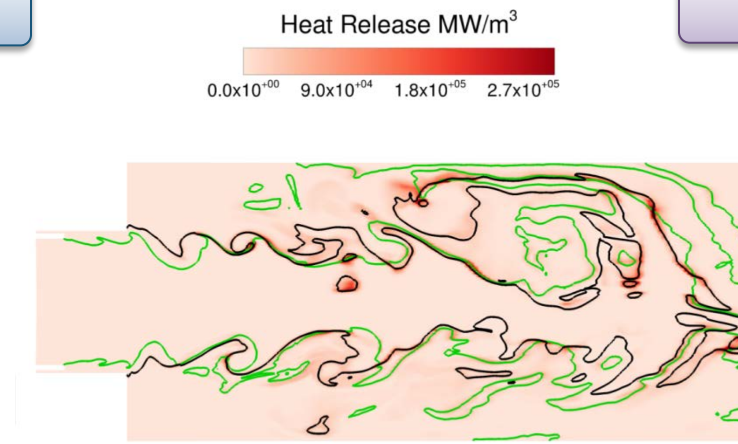

30 %

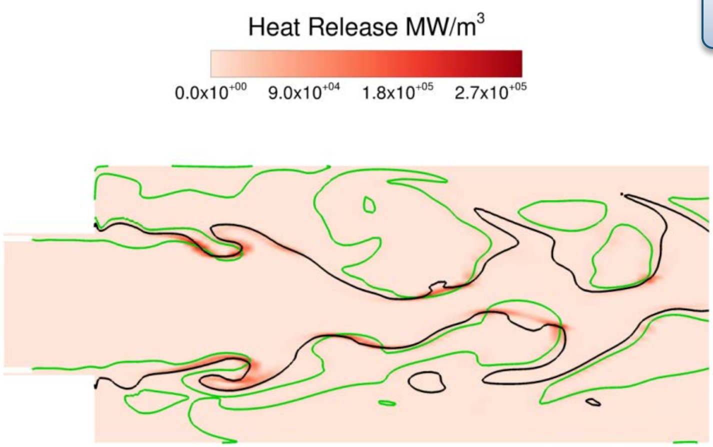

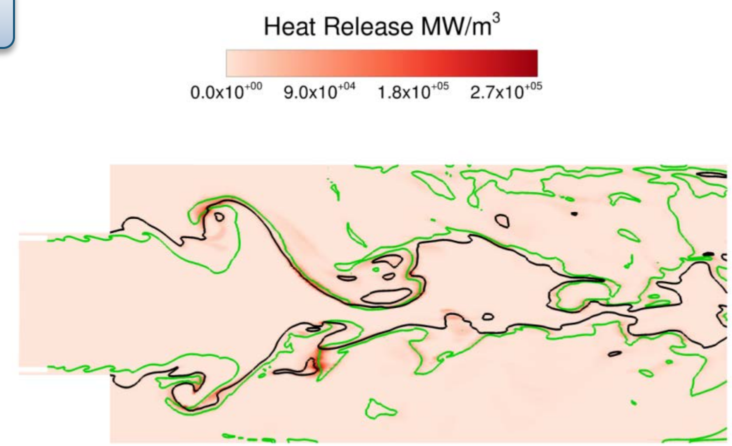

Heat Release Cycle – Part II

DES

60 %

LES

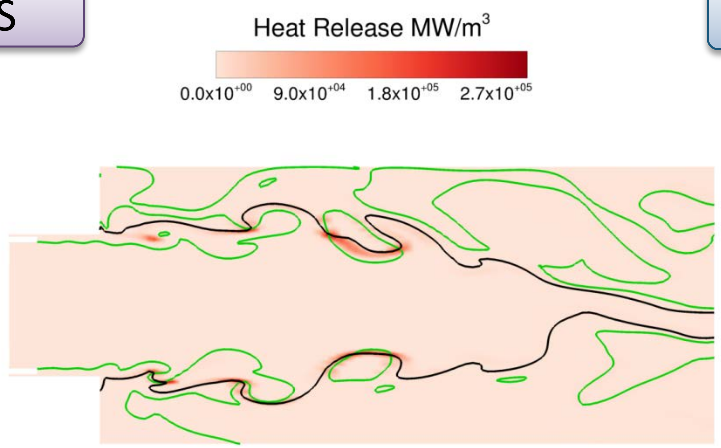

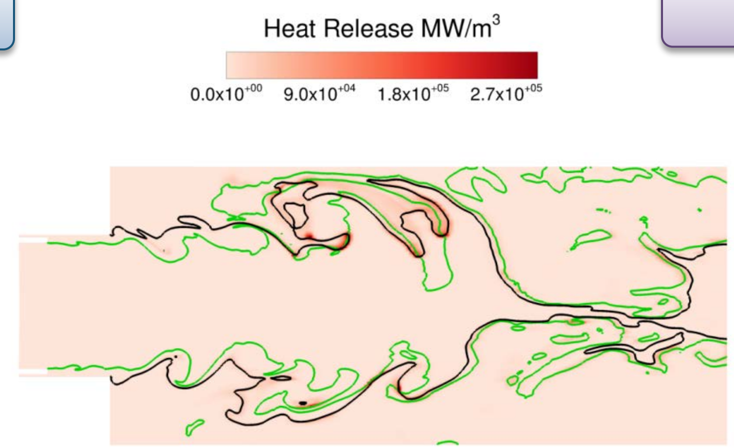

90 %

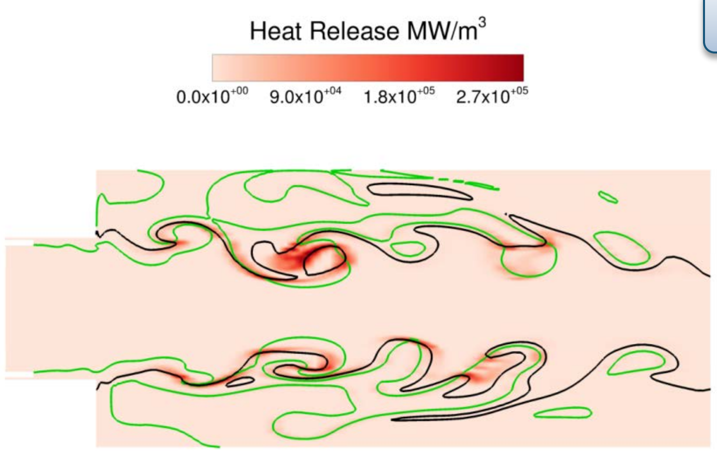

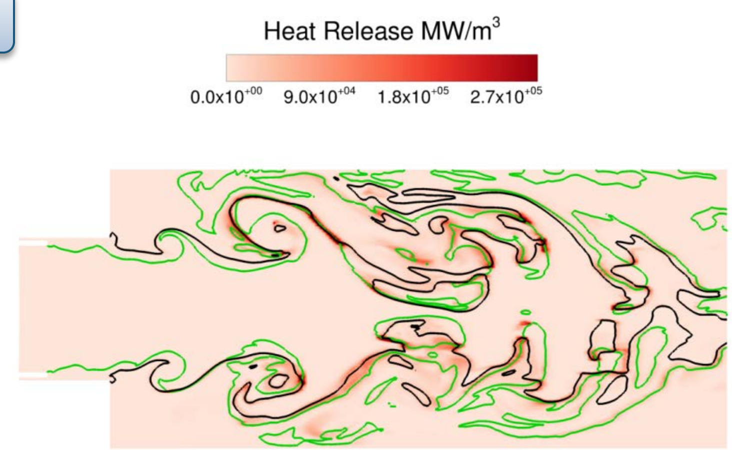

Summary & Conclusions

Both LES and DES area capable of simulating self-excited combustion instability

Agreement between the simulations and experiments for the unstable case was good

Cyclic Heat release was captured

LES had a delayed reignition, likely responsible for the higher amplitudes

Cyclic Heat release was captured along with reignition event

Some differences in predictions are due to differences in the grids

The marginally stable case proved more difficult

No apparent winner, both approaches have strengths and weaknesses